2017

How are coastal benthos fed?

James Waples
University of Wisconsin - Milwaukee, jwaples@uwm.edu

Harvey A. Bootsma

J. Val Klump

Recommended Citation

This is the peer reviewed version of the following article: Waples JT, Bootsma HA, Klump VJ (2017) How are coastal benthos fed?. Limnology and Oceanography Letters 2(1): 18–28, which has been published in final form at http://dx.doi.org/10.1002/lol2.10033. This article may be used for non-commercial purposes in accordance with Wiley Terms and Conditions for Self-Archiving.

LIMNOLOGY AND OCEANOGRAPHY
Letters

ASLO
Open Access

Limnology and Oceanography Letters 2, 2017, 18–28

doi: 10.1002/lol2.10033

LETTER

How are coastal benthos fed?

James T. Waples, Harvey A. Bootsma, J. Val Klump*
School of Freshwater Sciences, University of Wisconsin-Milwaukee, 600 East Greenfield Avenue, Milwaukee, WI 53204

Scientific Significance Statement

Benthic communities in nearly all aquatic systems are regulated in part by the flux of particulate organic material from overlying waters. In calm waters, this flux is mainly driven by particle settling; however, in shallow, energetic waters, where many suspension feeders live, advection and turbulent diffusion can influence particle flux, and their effect on particle delivery to benthic communities is not well quantified. In this study, we use naturally occurring radionuclides to show that advective onshore transport and rapid convective mixing increased particulate organic carbon flux to the nearshore benthos by a factor of ~15. This is the first study to show the importance of these delivery mechanisms to benthic communities in freshwater systems.

Abstract

Water movement can influence the distribution of benthos, in part, by increasing food delivery; however, the impact of advective transport and turbulent diffusion on organic matter flux to nearshore benthic communities is not well quantified. In this study, we measured the vertical particulate organic carbon (POC) and particulate phosphorus (PP) flux in nearshore Lake Michigan using two naturally occurring daughter/parent radionuclide pairs (^{234}Th/^{238}U and ^{90}Y/^{90}Sr) and compared these fluxes to coincident benthic chamber estimates of respiration and total phosphorus efflux by quagga mussels on the lakebed. We found that advective onshore transport and vertical convective mixing increased POC and PP flux to the nearshore benthos by a factor of ~15 and ~30 over offshore trap-derived estimates of flux. From these results, we hypothesize that high benthos population densities are related to an edge effect created when the dominant mechanism of particle delivery transitions from gravitational settling to convection.

Introduction

Benthic communities in nearly all aquatic systems are regulated in part by the flux of particulate organic material (POM) from overlying waters. In calm waters, this flux is mainly driven by particle settling, yet in shallow, energetic waters, advection and turbulent diffusion also can influence particle flux. Because water movement can increase the delivery of POM to benthic organisms, it has been correlated with enhanced benthic community metabolism and production (Nixon et al. 1971; Wildish and Kristmanson 1997; Dame and Prins 1998; Herman et al. 1999; Menge et al. 2003). Unfortunately, the effect of water movement on POM flux is difficult to measure directly, particularly in energetic coastal (margin) systems, and thus the empirical relationship between water movement, food delivery, and benthic food consumption remains poorly defined.

*Correspondence: jwaples@uwm.edu

Author Contribution Statement: JTW and HAB designed the study approach and conducted the field work. Radionuclide measurements were made by JTW (β, α) and JVK (γ). HAB conducted nutrient concentration measurements and benthic chamber experiments. JTW wrote the manuscript with input from all co-authors.

Data Availability Statement: Data available from the Dryad Digital Repository at http://dx.doi.org/10.5061/dryad.q14n6

Additional Supporting Information may be found in the online version of this article.

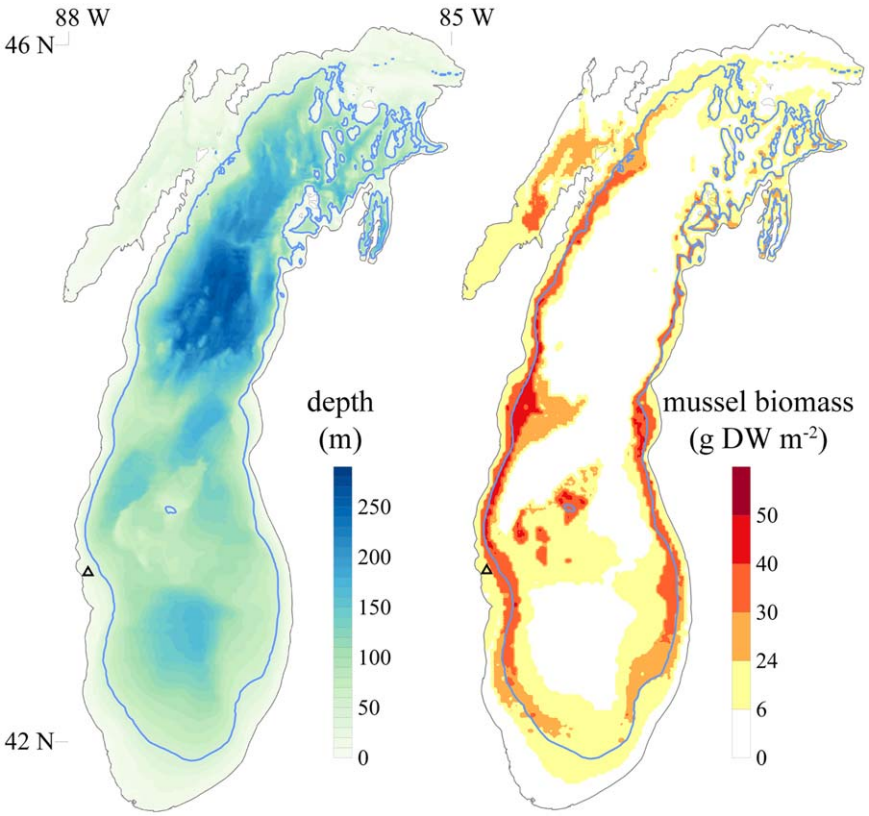

Fig. 1. Lake Michigan bathymetry (left); 2010 dreissenid mussel biomass (right). Study site (GC20) shown as triangle. Blue line shows 50 m isobath. Mussel biomass redrawn from data by Rowe et al. (2015), where mussel ash free dry weight (AFDW) converted to dry weight (DW) using ratio of 0.88 : 1.

Estimates of POM flux from the water column generally have relied on use of the moored sediment trap, but in shallow and turbulent water, sediment trap collection rates are poor proxies for particle flux (Schelske et al. 1984; White 1990; Storlazzi et al. 2011). Moreover, as turbulence increases, particle delivery to the bottom is controlled by convective mixing, not particle settling (Lick 1982). Consequently, trap-derived estimates of food delivery are often lower than what is required to support observed benthic respiration (Klerks et al. 1996; Andersson et al. 2004; van Oevelen et al. 2009; Mosley and Bootsma 2015).

We examined this apparent mismatch between trap-derived POM flux and benthic respiration in Lake Michigan. Pelagic primary production in Lake Michigan (58,000 km^2) is taken as $\sim$140 g C m^{-2} a^{-1} (Fee 1973; Fahnenstiel et al. 2016), of which 5–20% is exported to organisms living on the lake bottom (Eadie et al. 1984; Baines et al. 1994). The benthos of Lake Michigan are dominated by invasive quagga mussels (*Dreissena rostriformis bugensis*) (Evans et al. 2011; Rowe et al. 2015). Conservative oxygen consumption rates by quagga mussels ($\sim$0.01 mmol O_2 g DW^{-1} h^{-1}; Tyner et al. 2015) and an O_2/C molar respiratory quotient of 1 : 1.1 (Tyner et al. 2015) suggest a maximum (shell-free) biomass carrying capacity of $\leq$6 g DW m^{-2} at an export efficiency of 5% (Fig. 1, white area) to $\leq$24 g DW m^{-2} at an export efficiency of 20% (Fig. 1, white and yellow areas). Higher mussel densities along Lake Michigan's coast require a greater supply of food (Fig. 1, orange and red areas). If the distribution of benthic suspension feeding communities can be interpreted as an indication of POM availability (Herman et al. 1999; Rutgers van der Loeff et al. 2002), then how are these coastal mussels fed?

To resolve this issue, it will be necessary to measure POM flux and other particle-mediated transport in shallow systems confounded by water movement and boundary layer interactions. Recent studies have shown that naturally occurring radionuclides can be used to quantify particle flux, and, just as importantly, distinguish physical processes that are driving particle transport (Waples 2015).

Waples (2015) used two naturally occurring daughter/parent radionuclide pairs of $^{234}Th/^{238}U$ and $^{90}Y/^{90}Sr$ to show that convective mixing requires new formulation for the use of radionuclides as proxies for particle flux in shallow water. To test if this new approach to measuring particle flux resolves the apparent mismatch between POM flux and benthic respiration in Lake Michigan, our objectives in this study were to: (1) use the $^{234}Th/^{238}U$ and $^{90}Y/^{90}Sr$ tracer pairs to quantify the water column flux of particulate organic

carbon (POC) and particulate phosphorus (PP) to the nearshore lakebed, and (2) compare the flux of nutrients from the water column with coincident in situ benthic chamber estimates of quagga mussel oxygen consumption and P excretion.

Methods

Study site

The field survey took place at a shallow (~22 m) site on the western shore of southern Lake Michigan (Lat: 42° 59.1600 N, Long: 87° 47.9284 W) identified as station "GC20" by Waples (2015). The lakebed in this region is non-depositional and mostly sand with cobble and boulders.

Water sample collection

Water samples (~50 L) for radionuclide measurements were collected by submersible pump from 3, 10, and 17 m depths on five occasions over a 21-day period (August 20–September 10, 2009). Separate water samples (~20 L) were also collected at each depth and sample time and filtered through Whatman pre-ashed GF/F filters (0.7 μm) to analyze POC and PP.

Radionuclide analysis

Large-volume water samples were weighed and filtered through nitrocellulose filters (0.45 μm, 293 mm, Millipore) within ~3 h of sample collection to separate the particle-bound (> 0.45 μm) nuclide fraction. Dissolved ^{234}Th and ^{90}Y fractions (< 0.45 μm) were then co-precipitated onto newly formed iron hydroxide and collected by filtration. Next, ^{234}Th and ^{90}Y on both particle-bound and dissolved fractions were separated and isolated on an ion-exchange column, transferred to counting plates by electrodeposition (^{234}Th) or iron hydroxide precipitation (^{90}Y), and beta-counted on a low background gas-flow proportional detector with anti-coincidence circuitry (G542 System, Gamma Products). Yield monitors of ^{229}Th and ^{88}Y (Eckert & Ziegler Isotope Products), which were added to the samples at the beginning of the measurement procedure, were counted by alpha and gamma spectrometry, respectively, to determine sample recovery. ^{90}Sr activity was determined by ^{90}Y analysis of water stored for > 14 days until secular equilibrium between ^{90}Y and ^{90}Sr was achieved. ^{238}U activity was measured in previous studies (Waples 2015) and assumed to be constant. Reported errors are counting errors (± SD). Detailed methodologies for measuring ^{234}Th and ^{90}Y are described by Waples et al. (2003) and Waples and Orlandini (2010).

Benthic chamber experiments

Mussel consumption of O_2 and excretion of total dissolved phosphorus (TDP) were measured in situ under a benthic chamber (volume: 1.45 L; benthic interface: 0.0189 m^2). The chamber was deployed by diver on four occasions for durations of ~1.7–3.0 hours on mussel-covered rocks and sealed with a weighted neoprene skirt after all visible benthic algae (*Cladophora*) were carefully removed by hand. O_2 was measured continuously through a port in the chamber using an oxygen electrode (YSI model 600R Sonde). Chamber water was withdrawn through another port by syringe for TDP analysis at the beginning and end of each chamber experiment. Manually operated stir-paddles allowed for gentle stirring inside of the benthic chamber and the sampling of homogenous chamber water.

After each experiment, all mussels within the chamber were collected and measured for shell length. Fifteen mussels of varying length were lyophilized for 48 h and measurements of shell length (L) and shell-free biomass (m) were fitted to the standard allometric equation $m = a \times L^b$, where m was expressed in units of milligrams dry weight (mg DW), L was expressed in units of millimeters (mm), and a and b were 0.0018 and 3.11, respectively ($r^2 = 0.955$). This relationship was then applied to all shell length measurements to calculate total mussel biomass for each chamber experiment. Estimates of mussel tissue biomass were also calculated using Nalepa et al.'s (2014) empirical relationship of $m = 0.00225 \times L^{2.968}$ ($r^2 = 0.85$, $n = 244$), where m was expressed as ash-free dry weight (AFDW). After converting AFDW to DW (1 g DW = 0.88 g AFDW because the combusted sample ash weight is subtracted from the dry weight to obtain AFDW; Nalepa et al. 1993), the two calculations of mussel biomass differed by < 3%.

Organic carbon analysis

Filters for POC analysis were acidified with HCl (0.6 M) and rinsed with distilled water to remove inorganic C. Then, POC was measured using an isotope ratio mass spectrometer (Finnigan MAT delta S IRMS) with an elemental analyzer frontend and ConFlo II interface (Thermo Fisher Scientific, Waltham, MA). Replicate analyses ($n = 2$) are reported as mean ± MAD (mean absolute deviation). Acetanilide control samples (71.09% C; Costech Analytical Technologies) were run to ensure instrument calibration.

Phosphorus analysis

PP samples were converted to soluble reactive phosphorus (SRP) by combustion (550°C for 2 h) followed by heated digestion (1 M HCl and deionized water) at 105°C for 1.5 h. TDP samples were converted to SRP by digestion (2 M H_2SO_4 and H_2O_2) followed by a 2-h exposure to UV light in a photo-oxidizer. SRP was measured using the molybdate-ascorbic acid method (Stainton et al. 1977), with absorbance measured at 885 nm using a 10 cm path length. Replicate analyses ($n = 2$) are reported as ± MAD. Phosphorus standard curves were prepared using calibrated phosphorus standards (RICCA Chemical Company).

Ancillary data

Water currents were measured with a bottom-mounted SonTek ADP (1000 kHz; averaging interval: 60 s, profiling interval: 600 s, cell resolution: 1 m). Moored YSI sondes

located 1 m below surface and ~1 m above bottom measured the temperature and turbidity. Measurements were recorded throughout the study period.

Calculation of particulate flux

The $^{234}Th/^{238}U$ radionuclide pair has been used extensively to measure the export of sinking particles from the surface ocean (Waples et al. 2006, and references therein); however, its use as a particle tracer in coastal and near-bottom water has been less frequent due to the complicating influences of horizontal transport and ^{234}Th interaction with bottom sediment (e.g., Gustafsson et al. 1998; Rutgers van der Loeff et al. 2002; Savoye et al. 2006). The use of ^{90}Y and its parent ^{90}Sr (sourced from weapons fallout) as a proxy for particle flux is relatively new (Waples and Orlandini 2010).

Using $^{234}Th/^{238}U$ and $^{90}Y/^{90}Sr$ radionuclide pairs to measure particle flux is conceptually simple (Savoye et al. 2006). Both ^{238}U ($t_{1/2} = 4.5 \times 10^9$ a) and ^{90}Sr ($t_{1/2} = 28.8$ a) are conservative in aquatic systems, while both daughters ^{234}Th ($t_{1/2} = 24.1$ d) and ^{90}Y ($t_{1/2} = 64$ h) are particle-reactive. The daughter nuclide will preferentially bind to particles in the water column and—in a low-energy system—settle by gravity (Fig. 2a). Under 1-D steady-state conditions, the rate of removal of the daughter nuclide from the water column can be calculated by measuring the disequilibrium or difference in parent nuclide activity (A_P) and total (dissolved + particle-bound) daughter nuclide activity (A_D) (Fig. 2b). Because the production rate of A_D is known, the flux of A_D from the water column ($J\,A_D$) can be calculated at any depth z as the difference between the parent and daughter nuclide inventory ($A_P - A_D$; Bq m^{-2}) × the daughter nuclide decay constant (λ, d^{-1}):

$$J\,A_D = \lambda(A_P - A_D). \quad (1)$$

The flux of any particle constituent (*J mass*; e.g., *J POC*, g m^{-2} d^{-1}) can then be calculated as the product of the daughter nuclide flux (Bq m^{-2} d^{-1}) and the ratio of the constituent mass and daughter nuclide activity on particles at depth z ($mass/A_D^{part}$, g Bq^{-1}):

$$J\,mass = J\,A_D \times \frac{mass}{A_D^{part}}. \quad (2)$$

In shallow coastal waters, however, 1-D steady-state conditions are rare. In this study, along the western shore of Lake Michigan, Waples (2015) used a 2-D non-steady-state approach to calculate the vertical water column fluxes of both ^{234}Th and ^{90}Y as:

$$J\,A_D = \lambda(A_P - A_D) - \frac{\partial A_D}{\partial t} - u\frac{\partial A_D}{\partial x} + K_x\frac{\partial^2 A_D}{\partial x^2} + R \quad (3)$$

where the first term on the RHS of Eq. 3 represents the local growth of A_D due to radioactive decay; the second term

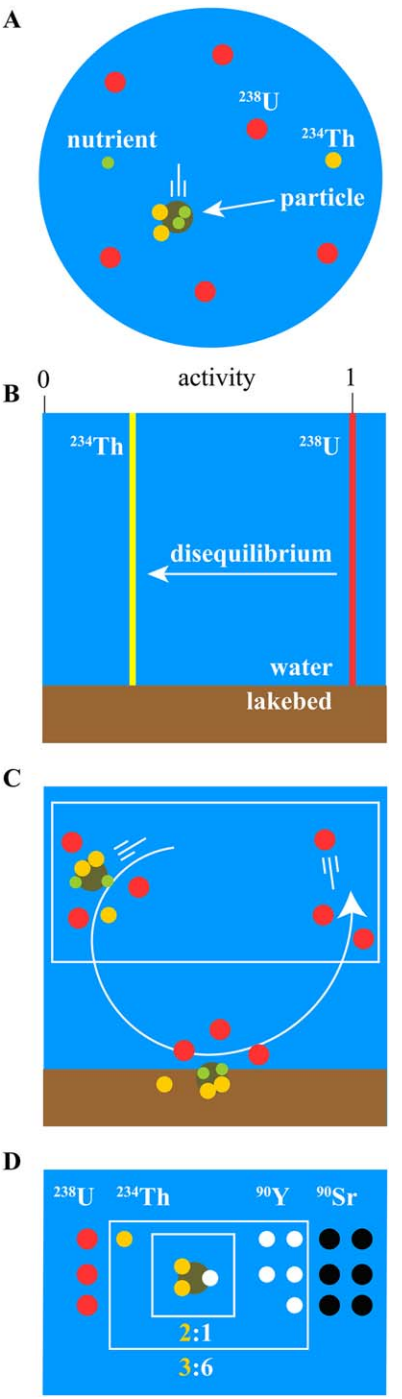

Fig. 2. Mechanisms of reactive nuclide scavenging in shallow water. (**a**) ^{234}Th can sorb to settling particles. (**b**) Removal of ^{234}Th from water column leads to disequilibrium between ^{234}Th and its conservative parent ^{238}U. (**c**) ^{234}Th can also be scavenged by direct sorption to bottom sediments through convection (vertical advection + turbulent diffusion). Mass flux calculation derived from measurements in water column [white box] sensitive to scavenging mechanism. (**d**) If two particle reactive tracers measured ($^{234}Th:^{238}U$ and $^{90}Y:^{90}Sr$), end-member $^{234}Th/^{90}Y$ flux ratios from water proportional to (*i*) the daughter nuclide ratio on particles if scavenging dominated by particle settling, or (*ii*) the total daughter nuclide ratio if removal dominated by complete bottom scavenging.

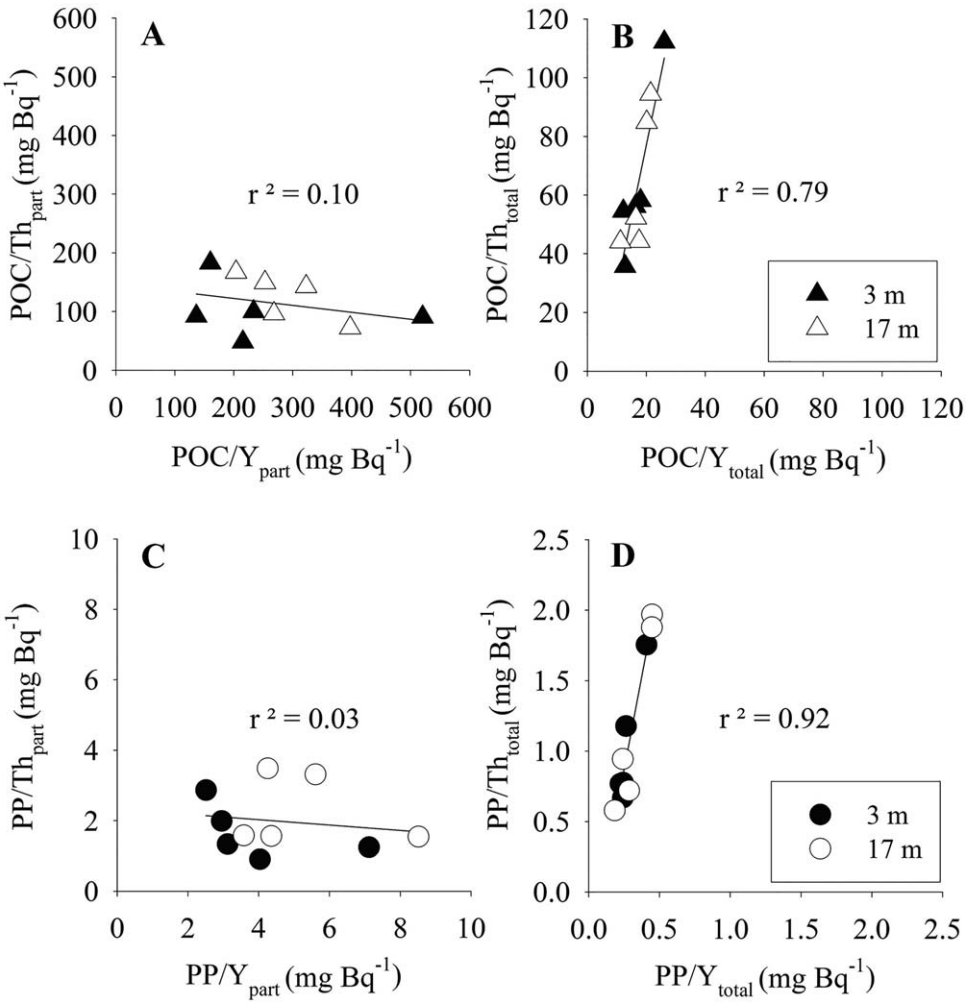

Fig. 3. Particle nutrient mass and nuclide activity ratios at 3 and 17 m depth over five sampling intervals. (**a**) POC/nuclide ratios using particle-bound nuclide activity. (**b**) POC/nuclide ratios using total (dissolved + particle bound) nuclide activity. (**c**) PP/nuclide ratios using particle-bound nuclide activity. (**d**) PP/nuclide ratios using total nuclide activity. R^2 coefficients for linear regression analysis.

represents the non-steady-state change in A_D over time; the third and fourth terms represent advective and turbulent diffusive transport of A_D in the cross-shore (horizontal) direction; and the last term represents the flux of A_D reintroduced to the water column through resuspension. Specific terms include the daughter nuclide decay constant ($\lambda_{Th} = 0.02876\ d^{-1}$, $\lambda_Y = 0.25993\ d^{-1}$), current velocities in the offshore horizontal (u) direction, and turbulent diffusion in the cross-shore horizontal (K_x) direction. The solutions and supporting data for each term of Eq. 3 are given by Waples (2015).

Using radionuclides to calculate mass flux is further complicated in shallow coastal waters because the daughter nuclide also can sorb directly to bottom or near-bottom sediment by vertical convection (advection + turbulent diffusion) (Fig. 2c). However, this scavenging mechanism can be identified by using two radionuclide tracers with differing particle reactivities (Waples 2015). If particle removal is controlled by settling, then the water column $^{234}Th/^{90}Y$ flux ratio will equal the $^{234}Th/^{90}Y$ activity ratio on settling particles (e.g., 2 : 1 in Fig. 3d), where:

$$\frac{J^{234}Th}{J^{90}Y} = \frac{^{234}Th^{part}}{^{90}Y^{part}} \tag{4}$$

If, however, particle removal is controlled by convection with complete scavenging at the sediment/water interface, then the water column $^{234}Th/^{90}Y$ flux ratio will equal the total $^{234}Th/^{90}Y$ activity ratio in the water column (e.g., 3 : 6 in Fig. 3d), where:

$$\frac{J^{234}Th}{J^{90}Y} = \frac{^{234}Th}{^{90}Y} \tag{5}$$

In this nearshore study, evidence suggested total scavenging of both ^{234}Th and ^{90}Y at depth, and that the delivery of both nuclides and particles was controlled by convection

Table 1. Calculation of particulate organic carbon (POC) and particulate phosphorus (PP) fluxes (± propagated error).

Time span (2009)	20–25 August	25–28 August	28–31 August	31 August–10 September	20 August–10 September
Duration (days)	4.9	3.0	3.0	10.0	21.0
^{234}Th flux (Bq m^{-2} d^{-1})*	17	32	72	3	
^{90}Y flux (Bq m^{-2} d^{-1})*	46	95	249	12	
POC/^{234}Th (mg Bq^{-1})†	45 ± 5	44 ± 4	61 ± 4	89 ± 5	
^{234}Th derived POC flux (mg m^{-2} d^{-1})‡	825 ± 87	1429 ± 135	4392 ± 309	279 ± 16	
POC/^{90}Y (mg Bq^{-1})†	17.0 ± 1.8	13.7 ± 1.4	14.9 ± 1.1	20.8 ± 1.3	
^{90}Y derived POC flux (mg m^{-2} d^{-1})‡	785 ± 85	1307 ± 130	3697 ± 283	254 ± 16	
Average POC flux (mg m^{-2} d^{-1})§	805 ± 61	1368 ± 94	4045 ± 210	267 ± 11	1100 ± 100‖
PP/^{234}Th (mg Bq^{-1})†	0.65 ± 0.02	0.83 ± 0.03	1.28 ± 0.04	1.92 ± 0.06	
^{234}Th derived PP flux (mg m^{-2} d^{-1})‡	11 ± 0.3	27 ± 0.9	93 ± 2.9	6 ± 0.2	
PP/^{90}Y (mg Bq^{-1})†	0.23 ± 0.01	0.26 ± 0.01	0.31 ± 0.01	0.45 ± 0.02	
^{90}Y derived PP flux (mg m^{-2} d^{-1})‡	11 ± 0.4	25 ± 1.2	78 ± 3.4	5 ± 0.2	
Average PP flux (mg m^{-2} d^{-1})§	11 ± 0.3	26 ± 0.7	85 ± 2.3	6 ± 0.2	21 ± 1‖

* Nuclide fluxes from Waples (2015).
† Average nutrient/total nuclide ratios calculated using first and second date listed in time span (see Table S1).
‡ Particulate nutrient flux calculated as product of nuclide flux and nutrient mass/nuclide activity ratio.
§ Average of ^{234}Th and ^{90}Y derived nutrient flux.
‖ Time weighted average.

rather than gravitational settling (Waples 2015). Accordingly, mass fluxes were calculated as:

$$J\,mass = J\,A_D \times \frac{mass}{A_D} \quad (6)$$

where $mass/A_D$ is the ratio of particle constituent mass-to-total daughter nuclide activity at depth z.

Results

POC and PP fluxes from the water column

Gross (vertical) fluxes of ^{234}Th and ^{90}Y at 20 m depth were calculated by Waples (2015) using Eq. 3 and are presented in Table 1. ^{234}Th fluxes ranged from 3 to 72 Bq m^{-2} d^{-1}. ^{90}Y fluxes ranged from 12 to 249 Bq m^{-2} d^{-1}. The mean time-weighted nuclide fluxes over the 21-day experiment were ~21 Bq ^{234}Th m^{-2} d^{-1} and ~66 Bq ^{90}Y m^{-2} d^{-1}, resulting in a $J\,^{234}Th/J\,^{90}Y$ flux ratio of ~0.31.

POC and PP mass/activity ratios (Table S1, Fig. S1) were calculated for both particle-bound ($mass/A_D^{part}$, Fig. 3a,c) and total ($mass/A_D$, Fig. 3b,d, Table 1) nuclide activities. Linear relationships between nutrient mass/^{234}Th activity and nutrient mass/^{90}Y activity over time and depth were only significant for $mass/A_D$ ratios (POC: $p = 0.0005$, $r^2 = 0.79$; PP: $p < 0.0001$, $r^2 = 0.92$), indicating that consistent scavenging mechanisms were acting on $mass/A_D$ ratios over the entire water column for the duration of the experiment. Inverse $A_D/mass$ relationships between ^{234}Th activity/nutrient mass and ^{90}Y activity/nutrient mass (not shown) also showed that ^{234}Th/^{90}Y activity ratios for POC (0.28 ± 0.08; $p = 0.008$, $r^2 = 0.60$) and PP (0.37 ± 0.06; $p = 0.0004$, $r^2 = 0.81$) were similar to the $J\,^{234}Th/J\,^{90}Y$ flux ratio of ~0.31, indicating bottom scavenging and convective control of particle flux (see Eq. 5 vs. Eq. 4).

To calculate the vertical POC and PP fluxes (Eq. 6), we multiplied the daughter nuclide flux ($J\,A_D$) by the $mass/A_D$ ratio of particle constituent mass-to-total daughter nuclide activity at depth (Table 1). POC fluxes (Fig. 4a, black fill) ranged from 270 to 4000 mg m^{-2} d^{-1}, with a time-weighted mean flux of 1100 ± 100 mg C m^{-2} d^{-1}. For comparison, satellite-derived estimates from 2010 to 2013 of nearshore (0–30 m), summertime primary production—calibrated against seasonal productivity measurements based on ^{14}C incubations—were 200–800 mg C m^{-2} d^{-1} (Fahnenstiel et al. 2016; Fig. 4a, gray lines). PP fluxes ranged from 5.5 to 85 mg m^{-2} d^{-1}, with a time-weighted mean flux of 21 ± 1 mg P m^{-2} d^{-1} (Fig. 4b, black fill). Changes in flux over time were primarily due to variations in onshore current (Waples 2015).

Mussel oxygen consumption and phosphorus excretion

Mussel population densities on rock surfaces averaged 20,900 ± 3600 mussels m^{-2} ($n = 4$ sites). Mussel tissue biomass was 117 ± 39 g DW m^{-2} (Table S2).

Oxygen consumption rates ranged from 0.24 to 1.69 mg O_2 g DW^{-1} h^{-1} (Fig. S2, Table S2). TDP excretion rates ranged from 2.0 to 7.1 μg TDP g DW^{-1} h^{-1} (Table S2). To determine the areal fluxes of mussel O_2 consumption and P

excretion, we multiplied the mussel mass-specific flux rates by the local mussel population density (Table S2), resulting in areal oxygen consumption rates ranging from 660 ± 220 to 4800 ± 1600 mg O_2 m^{-2} d^{-1} (Fig. 4c), with areal TDP excretion rates ranging from 5.8 ± 1.9 to 20 ± 7 mg P m^{-2} d^{-1} (Fig. 4d).

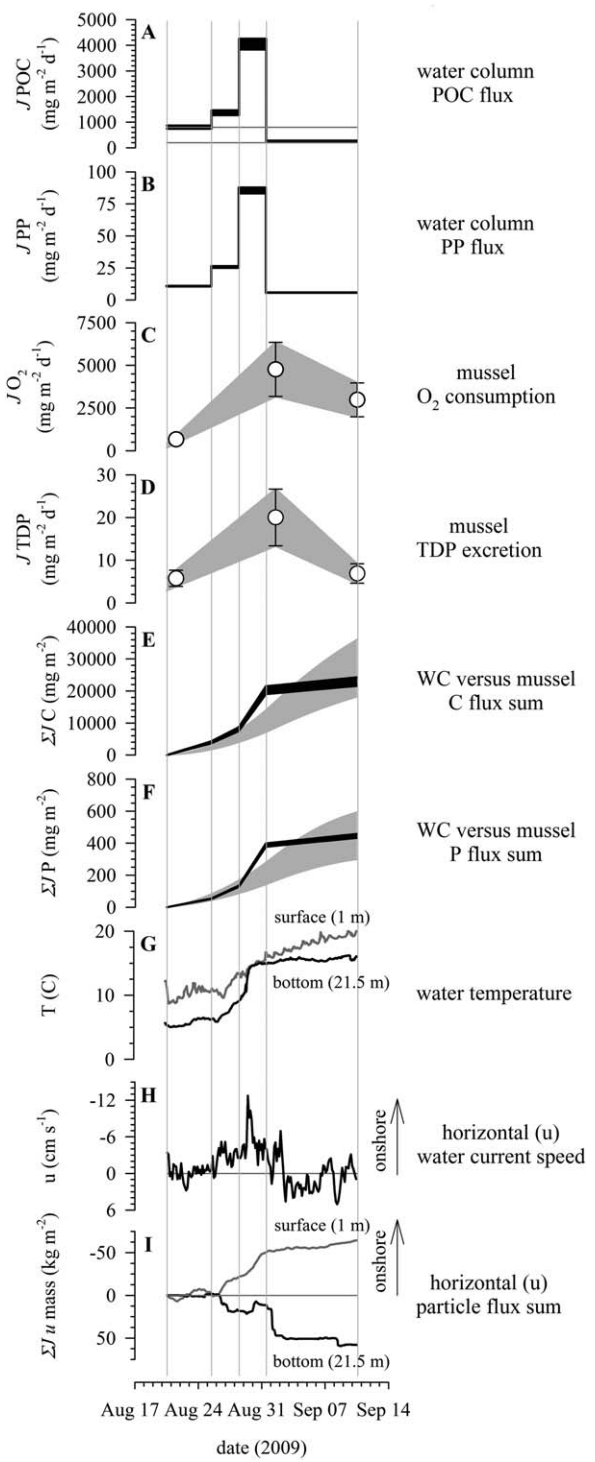

To estimate carbon respiration by mussels, we multiplied the areal mussel O_2 consumption rates by a molar respiratory quotient of 1 : 1.1 (O_2/C; Tyner et al. 2015). Respired carbon fluxes from mussels were 300 ± 100; 2000 ± 700; and 1200 ± 400 mg C m^{-2} d^{-1} on 21 August, 1 September, and 10 September, respectively. Daily respired carbon fluxes from mussels were estimated by linear interpolation and summed to give a total flux of 27,000 ± 9000 mg C m^{-2}, or 1300 ± 400 mg C m^{-2} d^{-1} (Fig. 4e, gray fill). By comparison, summed POC fluxes from the water column were 23,000 ± 2000 mg C m^{-2}, or 1100 ± 100 mg C m^{-2} d^{-1} (Fig. 4e, black fill).

To estimate total phosphorus (TP) efflux from mussels, we multiplied areal mussel TDP excretion rates by an empirically derived mussel TDP : TP efflux ratio of 1 : 1.67 (Mosley and Bootsma 2015). TP fluxes from mussels were 10 ± 3, 33 ± 11, and 11 ± 4 mg P m^{-2} d^{-1} on 21 August, 1 September, and 10 September, respectively. Daily mussel TP fluxes were estimated by linear interpolation and summed to give a total flux of 446 ± 148 mg P m^{-2}, or 21 ± 7 mg P m^{-2} d^{-1} (Fig. 4f, gray fill). Summed PP fluxes from the water column were 445 ± 22 mg P m^{-2}, or 21 ± 1 mg P m^{-2} d^{-1} (Fig. 4f, black fill).

Ancillary physical measurements

To provide some context of the physical environment in which these radionuclide and nutrient measurement were made, we include measurements of water column temperature (Fig. 4g) and shore normal currents (Fig. 4h), and estimates of shore normal particle transport (Fig. 4i).

Depth-integrated horizontal (shore normal) water currents flowed toward shore, on average, at $u = -847$ m d^{-1} over the course of the 21-day experiment (Fig. 4h). Highest currents were again toward shore, averaging $u = -4596$ m d^{-1} over the 28–31 August time interval. Shore normal currents flowed offshore, however, at $u = 333$ m d^{-1} during the time interval 31 August to 10 September.

To estimate horizontal (shore-normal) particle mass transport, we multiplied sonde turbidity measurements at the surface (1 m) and depth (21.5 m) by shore-normal currents at

Fig. 4. Flux summary. Nuclide sampling intervals separated by vertical gray lines. (**a**) POC flux from water column. Horizontal gray lines show range of net primary production. (**b**) PP flux from water column. (**c**) Benthic chamber measurement of O_2 consumption by mussels. (**d**) Benthic chamber measurement of TDP excretion by mussels. (**e**) Carbon flux sum from water column (black fill) and mussels carbon respiration (gray fill). Mussel O_2 : C respiration conversion 1 : 1.1 molar ratio (Tyner et al. 2015). (**f**) PP flux sum from water column (black fill) and mussels TP efflux sum (gray fill). Mussel efflux TDP : TP conversion 1 : 1.67 (Mosley and Bootsma 2015). (**g**) Water temperature measured 1 m below surface and 1 m above bottom. (**h**) Depth averaged (2–19 m) horizontal (u = shore normal) water currents. Negative values indicate shoreward transport. (**i**) Horizontal (shore normal) particle mass flux sum through 1 m^2 cell at surface and depth.

surface (2 m) and depth (19 m), and assumed 1 NTU ≈ 1 g SPM (suspended particulate matter) m^{-3}. While we cannot budget cross-shore transport with these data, the data show that surface material flowed onshore, bottom material flowed offshore, and onshore flux was temporally disconnected from offshore flux (Fig. 4i).

Discussion

C and P fluxes

Carbon and phosphorus fluxes from the water column (1100 ± 100 mg C m^{-2} d^{-1}, 21 ± 1 mg P m^{-2} d^{-1}) were concordant with estimates of carbon respiration and phosphorus efflux by mussels (1300 ± 400 mg C m^{-2} d^{-1}, 21 ± 7 mg P m^{-2} d^{-1}, Fig. 4e,f). ^{234}Th and ^{90}Y disequilibria integrated scavenging rates on the time and space scales of days and kilometers while mussel respiration and excretion rates were local (h, m) in scale. Nevertheless, the nuclide-derived fluxes from the water column represent a gross flux of what is presented to the lake bottom, and a community of filter feeders at carrying capacity might be expected to use this flux fully. Some proof of this is provided by the concordance we observed between ^{234}Th and ^{90}Y flux from the water column and ^{234}Th and ^{90}Y efflux from mussels on 10 September (Waples 2015).

Even more interesting–and pertinent to the central question of this article—is that both water column and mussel fluxes of organic and respired carbon were up to ~6 times higher than Fahnenstiel et al.'s (2016) estimate of pelagic primary production. Benthic primary production is a potential source of energy for benthic organisms. However, benthic production in nearshore Lake Michigan is dominated by a periphyton assemblage composed primarily of the macroalgae *Cladophora* and associated epiphytic diatoms. In our study area, δ^{13}C ratios of food web components indicated that quagga mussels feed on phytoplankton, and there is virtually no contribution of benthic algae to their diet (Turschak and Bootsma 2015). If quagga mussels are fed by POM produced in the water column, and our flux measurements are correct, then local demand must be supplemented by lateral transport.

Rates of quagga mussel oxygen consumption and phosphorus excretion were in general agreement with literature values. Mussel oxygen consumption (0.24–1.69 mg O_2 g DW^{-1} h^{-1}) compared well with Tyner et al.'s (2015, and references therein) ex situ (laboratory) measurements of 0.23–2.27 mg O_2 g DW^{-1} h^{-1}. Rates of TDP excretion (2.0–7.1 μg P g DW^{-1} h^{-1}) agreed with Mosely and Bootsma's (2015) estimates of ~3–6 μg P g DW^{-1} h^{-1}.

Nuclide-derived POC and PP fluxes in this nearshore study were, e.g., ~15 and ~30 times higher than Eadie et al.'s (1984) trap-derived estimates of ~75 mg C m^{-2} d^{-1} and ~0.7 mg P m^{-2} d^{-1} in offshore waters; however, ^{234}Th and ^{90}Y fluxes from the water column were corroborated by measured nuclide inventories on the lakebed (Waples 2015). Furthermore, the use of $mass/A_D$ ratios in Eq. 6 (rather than $mass/A_D^{part}$ ratios in Eq. 2) results in *minimum* estimates of POC and PP flux, as Fig. 3 shows.

Offshore food source

Lateral food supplements may have come from tributary loading (e.g., Biddanda and Cotner 2002; Vanderploeg et al. 2010), alongshore advection, or the inflow of pelagic offshore waters, but the first two mechanisms are unlikely. Total phosphorus loading from the Milwaukee River (9 km to the northwest of our sampling site) averaged ~250 kg P d^{-1} in 2009 (Fillingham 2015). P fluxes in this study (~21 mg P m^{-2} d^{-1}) could have removed this tributary loading over a relatively small ~12 km^2 area. Likewise, alongshore currents generally flowed southward at our study site (Waples 2015), but supporting local mussel biomass with upshore production only shifts the question to how mussels further north are fed, as Fig. 1 illustrates.

Evidence for the importance of the onshore transport of offshore pelagic water was provided by measured water currents. POC and PP fluxes from the water column were higher with onshore flow than with offshore flow (Fig. 4, Waples 2015). More importantly, a previous study of ^{234}Th along a shore-normal (0–40 m depth) transect ~13 km north of our current study site revealed sediment + water column ^{234}Th inventories that were on average ~2.4 times higher than the supporting ^{238}U inventory, with site-specific ^{234}Th/^{238}U activity ratios as high as 12 (Waples and Klump 2013). Because the inventory of ^{234}Th activity cannot exceed the inventory of its parent ^{238}U activity in a 1-D system, ^{234}Th/^{238}U activity ratios > 1 along with the lack of any significant alongshore ^{234}Th gradient is an unequivocal signal of boundary scavenging and horizontal transport from offshore waters (Gustafsson et al. 1998).

The average contribution of onshore nuclide transport to local vertical nuclide flux was ~65% (Waples 2015). Applying the same percentage to POC flux suggests that an average of ~400 mg C m^{-2} d^{-1} was locally produced while the remaining flux of ~700 mg C m^{-2} d^{-1} was sourced from offshore waters. Similar findings of offshore support for coastal bivalves have been reported in marine systems (Dame and Prins 1998; Menge et al. 2003).

Vertical convection and benthos population density

The importance of vertical mixing on food delivery to benthos is well known. In this summertime study under mostly stratified conditions, vertical turbulent diffusion coefficients (K_z), derived from ^{234}Th and ^{90}Y fluxes by Waples (2015), averaged 1.8×10^{-3} m^2 s^{-1} (range: 3.5×10^{-4} m^2 s^{-1} to 6.6×10^{-3} m^2 s^{-1}) over the water column and correlated positively with onshore advection. These K_z values were ~100× greater than those found by Edwards et al. (2005) in Lake Erie, but in good agreement with boundary mixing rates observed by MacIntyre et al. (1999) in Mono

Lake, Lorke et al. (2008) in Lake Constance, and more recently by Troy et al. (2016) in Lake Michigan.

Scaling arguments by Lick (1982) relate the delivery time of water column particles to the bottom by turbulent diffusion (t_d) to gravitational settling (t_s) as:

$$\frac{t_d}{t_s} = \frac{W_s h}{2K_z} \quad (7)$$

where W_s is the settling velocity of the particle, and h is the water column depth. Using a settling velocity of ~ 1 m d^{-1} for detrital POC (Burns and Rosa 1980), the t_d/t_s delivery ratio at our study site averaged ~ 15 and exceeded 50 during periods with strong onshore advection. At some greater water column depth, Eq. 7 predicts that gravitational settling is eventually the dominant particle delivery mechanism. The water column depth at which this transition between delivery mechanisms takes place can be identified in future studies using the radionuclide tracer techniques we employed here.

We hypothesize that the transition between particle delivery mechanisms plays a role in benthos population density (Gili and Coma 1998; Shields and Hughes 2009), and that the high-population densities of filter-feeding benthos along basin margins correspond with the deepest depth at which particle delivery to the bottom is enhanced year-round by both onshore advection and vertical turbulent mixing. Excessive turbulence may drive populations to deeper, calmer depths (Carney 2005), but where food and habitat are the only limiting factors, the advantage lies in close proximity to where the quantity and quality of POM flux is initially enhanced by vertical convection (Herman et al. 1999).

Conclusion

Food supplements to nearshore and coastal benthos from offshore pelagic waters are perhaps more commonplace than currently realized, especially in freshwater systems. In lakes as well as the ocean, vertical mixing is stronger along margins than it is in the interior, and elevated activities of radionuclides in margin sediments show that transport of material from the basin interior occurs (Crusius and Anderson 1995; Gustafsson et al. 1998; Lorke et al. 2008). In the same way that the distribution of benthic suspension feeding communities can be interpreted as an indication of POM availability, short-lived radionuclide inventories in sediments and benthic fauna might easily serve as a proxy for recent food delivery (Miller et al. 2000; Rutgers van der Loeff et al. 2002; Waples and Klump 2013). Radionuclide ratios can indicate the mechanism of particle delivery (Waples 2015). And nuclide inventories in excess of their local parent sources provide an unequivocal signal of lateral transport. Relating these measurements to water flow and benthos population densities can improve our understanding of how coastal benthos are fed.

References

Andersson, J. H., J. W. M. Wijsman, P. M. J. Herman, J. J. Middelburg, K. Soetaert, and C. Heip. 2004. Respiration patterns in the deep ocean. Geophys. Res. Lett. **31**: L03304. doi:10.1029/2003GL018756.

Baines, S. B., M. L. Pace, and D. M. Karl. 1994. Why does the relationship between sinking flux and planktonic primary production differ between lakes and oceans? Limnol. Oceanogr. **39**: 213–226. doi:10.4319/lo.1994.39.2.0213

Biddanda, B. A., and J. B. Cotner. 2002. Love handles in aquatic ecosystems: The role of dissolved organic carbon drawdown, resuspended sediments, and terrigenous inputs in the carbon balance of Lake Michigan. Ecosystems **5**: 431–445. doi:10.1007/s10021-002-0163-z

Burns, N. M., and F. Rosa. 1980. In situ measurement of the settling velocity of organic carbon particles and 10 species of phytoplankton. Limnol. Oceanogr. **25**: 855–864. doi:10.4319/lo.1980.25.5.0855

Carney, R. S. 2005. Zonation of deep biota on continental margins. Oceanograph. Mar. Biol. Ann. Rev. **43**: 211–278. doi:10.1201/9781420037449.ch6

Crusius, J., and R. F. Anderson. 1995. Sediment focusing in six small lakes inferred from radionuclide profiles, Paleolimnology **13**: 143–155. doi:10.1007/BF00678103

Dame, R, F., and T. C. Prins. 1998. Bivalve carrying capacity in coastal ecosystems. Aquat. Ecol. **31**: 409–421. doi:10.1029/2003GL018756

Eadie, B. J., R. L. Chambers, W. S. Gardner, and G. L. Bell. 1984. Sediment trap studies in Lake Michigan: Resuspension and chemical fluxes in the southern basin. J. Great Lakes Res. **10**: 307–321. doi:10.1016/S0380-1330(84)71844-2

Edwards, W. J., C. R. Rehmann, E. McDonald, and D. A. Culver. 2005. The impact of a benthic filter feeder: Limitations imposed by physical transport of algae to the benthos. Can. J. Fish. Aquat. Sci. **62**: 205–214. doi:10.1139/f04-188

Evans, M. A., G. Fahnenstiel, and D. Scavia. 2011. Incidental oligotrophication of North American Great Lakes. Environ. Sci. Technol. **45**: 3297–3303. doi:10.1021/es103892w

Fahnenstiel, G. L., M. J. Sayers, R. A. Shuchman, F. Yousef, S. A. Pothoven. 2016. Lake-wide phytoplankton production and abundance in the Upper Great Lakes: 2010–2013. J. Great Lakes Res. **42**: 619–629. doi:10.1016/j.jglr.2016.02.004

Fee, E. J. 1973. A numerical model for determining integral primary production and its application to Lake Michigan. J. Fish. Res. Bd. Can. **30**: 1447–1468. doi:10.1139/f73-235

Fillingham, J. H. 2015. Modeling Lake Michigan nearshore carbon and phosphorus dynamics. Ph.D. Dissertation. Univ. of Wisconsin-Milwaukee.

Gili, J. M., and R. Coma. 1998. Benthic suspension feeders: their paramount role in littoral marine food webs. Trends Ecol. Evol. **13**: 316–321. doi:10.1016/S0169-5347(98)01365-2

Gustafsson, Ö, K. O. Buesseler, W. R. Geyer, S. B. Moran, and P. M. Gschwend. 1998. An assessment of the relative importance of horizontal and vertical transport of particle-reactive chemicals in the coastal ocean. Cont. Shelf Res. **18**: 805–829. doi:10.1016/S0278-4343(98)00015-6

Herman, P. M. J., J. J. Middelburg, J. van de Koppel, C. H. R. Heip. 1999. Ecology of estuarine macrobenthos. Adv. Ecol. Res. **29**: 195–231. doi:10.1016/S0065-2504(08)60194-4

Klerks, P. L., P. C. Fraleigh, and J. E. Lawniczak. 1996. Effects of zebra mussels (*Dreissena polymorpha*) on seston levels and sediment deposition in western Lake Erie. Can. J. Fish. Aquat. Sci. **53**: 2284–2291. doi:10.1139/cjfas-53-10-2284

Lick, W. 1982. Entrainment, deposition, and transport of fine-grained sediments in lakes. Hydrobiologia **91**: 31–40. doi:10.1007/BF00940094

Lorke, A., L. Umlauf, and V. Mohrholz. 2008. Stratification and mixing on sloping boundaries. Geophys. Res. Lett. **35**: L14610. doi:10.1029/2008GL034607

MacIntyre, S., K. M. Flynn, R. Jellison, and J. R. Romero. 1999. Mixing and nutrient fluxes in Mono Lake, California. Limnol. Oceanogr. **44**: 512–529. doi:10.4319/lo.1999.44.3.0512

Menge, B. A., and others. 2003. Coastal oceanography sets the pace of rocky intertidal community dynamics. Proc. Natl. Acad. Sci. **100**: 12229–12234. doi:10.1073/pnas.1534875100

Miller, R. J., C. R. Smith, D. J. DeMaster, and W. L. Fornes. 2000. Feeding selectivity and rapid particle processing by deep-sea megafaunal deposit feeders: A ^{234}Th tracer approach. J. Mar. Res. **58**: 653–673. doi:10.1357/002224000321511061

Mosley, C. M., and H. Bootsma. 2015. Phosphorus recycling by profunda quagga mussels (*Dreissena rostriformis bugensis*) in Lake Michigan. J. Great Lakes Res. **41**: 38–48. doi:10.1016/j.jglr.2015.07.007

Nalepa T. F., J. F. Cavaletto, M. Ford, W. M. Gordon, and M. Wimrner. 1993. Seasonal and annual variation in weight and biochemical content of the zebra mussel, *Dreissena polymorpha*, in Lake St. Clair. J. Great Lakes Res. **19**: 541–552. doi:10.1016/S0380-1330(93)71240-X

Nixon, S. W., C. A. Oviatt, C. Rogers, K. Taylor, and C. A. Vogers. 1971. Mass and metabolism of a mussel bed. Oecologia **8**: 21–30. doi:10.1007/BF00345624

Rowe, M. D., D. R. Obenour, T. F. Nalepa, H. A. Vanderploeg, F. Yousef, and W. C. Kerfoot. 2015. Mapping the spatial distribution of the biomass and filter-feeding effect of invasive dreissenid mussels on the winter-spring phytoplankton bloom in Lake Michigan. Freshwater Biol. **60**: 2270–2285. doi:10.1111/fwb.12653

Rutgers van der Loeff, M. M., R. Meyer, B. Rudels, and E. Rachor. 2002. Resuspension and particle transport in the benthic nepheloid layer in and near Fram Strait in relation to faunal abundances and ^{234}Th depletion. Deep-Sea Res. I **49**: 1941–1958. doi:10.1016/S0967-0637(02)00113-9

Savoye, N., and others. 2006. ^{234}Th sorption and export models in the water column: A review. Mar. Chem. **100**: 234–249. doi:10.1016/j.marchem.2005.10.014

Schelske, C. L., B. J. Eadie, and G. L. Krausse. 1984. Measured and predicted fluxes of biogenic silica in Lake Michigan. Limnol. Oceanogr., **29**: 99–110. doi:10.4319/lo.1984.29.1.0099

Shields, M. A., and D. J. Hughes. 2009. Large-scale variation in macrofaunal communities along the eastern Nordic Seas continental margin: A comparison of four stations with contrasting food supply. Prog. Oceanograph. **82**: 125–136. doi:10.1016/j.pocean.2009.05.001

Stainton, M. P., M. J. Capel, and F. A. J. Armstrong. 1977. The chemical analysis of fresh water, 2nd ed., vol. 25, 166 p. Fish. Mar. Serv. Misc. Spec. Publ.

Storlazzi, C. D., M. E. Field, and M. H. Bothner. 2011. The use (and misuse) of sediment traps in coral reef environments: Theory, observations, and suggested protocols. Coral Reefs **30**: 23–38. doi:10.1007/s00338-010-0705-3

Troy, C., D. Cannon, Q. Liao, and H. Bootsma. 2016. Logarithmic velocity structure in the deep hypolimnetic waters of Lake Michigan. J. Geophys. Res. Oceans **121**: 949–965. doi:10.1002/2014JC010506

Turschak, B. A., and H. A. Bootsma. 2015. Lake Michigan trophic structure as revealed by stable C and N isotopes. J. Great Lakes Res. **41**: 185–196. doi:10.1016/j.jglr.2015.04.004

Tyner, E. H., H. A. Bootsma, and B. M. Lafrancois. 2015. Dreissenid metabolism and ecosystem-scale effects as revealed by oxygen consumption, J. Great Lakes Res. **41**: 27–37. doi:10.1016/j.jglr.2015.05.009

Van Oevelen, D., G. Duineveld, M. Lavaleye, F. Mienis, K. Soetaert, and C. H. R. Heip. 2009. The cold-water coral community as a hot spot for carbon cycling on continental margins: A food-web analysis from Rockall Bank (northeast Atlantic). Limnol. Oceanogr. **54**: 1829–1844. doi:10.4319/lo.2009.54.6.1829

Vanderploeg, H. A., J. R. Liebig, T. F. Nalepa, G. L. Fahnenstiel, and S. A. Pothoven. 2010. Dreissena and the disappearance of the spring phytoplankton bloom in Lake Michigan. J. Great Lakes Res. **36**: 50–59. doi:10.1016/j.jglr.2010.04.005

Waples J. T. 2015. Particle delivery to the benthos of coastal Lake Michigan. J. Geophys. Res. Oceans **120**: 8238–8250. doi:10.1002/2015JC011297

Waples, J. T., K. A. Orlandini, K. M. Weckerly, D. N. Edgington, and J. V. Klump. 2003. Measuring low concentrations of ^{234}Th in water and sediment. Mar. Chem. **80**: 265–281. doi:10.1016/S0304-4203(02)00118-4

Waples, J. T., and others. 2006. An introduction to the application and future use of ^{234}Th in aquatic systems. Mar. Chem. **100**: 166–189. doi:10.1016/j.marchem.2005.10.011

Waples, J.T., and K. A. Orlandini. 2010. A method for the sequential measurement of yttrium-90 and thorium-234 and their application to the study of rapid particle

dynamics in aquatic systems. Limnol. Oceanogr. Meth. **8**: 661–677. doi:10.4319/lom.2010.8.0661

Waples, J. T., and J. V. Klump. 2013. Vertical and horizontal particle transport in the coastal waters of a large lake: An assessment by sediment trap and thorium-234 measurements. J. Geophys. Res. Oceans **118**: 5376–5397. doi: 10.1002/jgrc.20394

White, J. 1990. The use of sediment traps in high-energy environments. Mar. Geophys. Res. **12**: 145–152. doi: 10.1007/BF00310569

Wildish, D. J., and D. D. Kristmanson. 1997. Benthic suspension feeders and flow. Cambridge Univ. Press.

Acknowledgments

We thank K. Weckerly and D. Szmania for water sampling assistance, E. Wilcox for nutrient analyses, and the captain and crew of the R.V. Neeskay for platform support. This research was supported by the National Science Foundation (OCE 1030558) and the University of Wisconsin-Milwaukee School of Freshwater Sciences. Support for in situ measurements of mussel metabolism was provided by Wisconsin Sea Grant (R/HCE-09) and the Milwaukee Metropolitan Sewerage District.

Submitted 03 August 2016
Revised 31 October 2016
Accepted 21 November 2016